Chinese Journal of Oceanology and Limnology
Vol. 22, No. 3, P. 299-305, 2004

Seasonal variability of thermocline in the Yellow Sea*

QIAO Fangli (乔方利), XIA Changshui (夏长水), SHI Jianwei (施建伟)†, MA Jian (马建), GE Renfeng (葛人峰), YUAN Yeli (袁业立)
(The First Institute of Oceanography, State Oceanic Administration (SOA), Qingdao 266061, China)
(Key Laboratory of Marine Science and Numerical Modeling (MASNUM), SOA, Qingdao 266061, China)
(†Guest Researcher of MASNUM, SOA, China)

Received Apr. 25, 2004; revision accepted May 28, 2004

Abstract Based on the MASNUM wave-tide-circulation coupled numerical model, seasonal variability of thermocline in the Yellow Sea was simulated and compared with in-situ observations. Both simulated mixed layer depth (MLD) and thermocline intensity have similar spatial patterns to the observations. The simulated maximum MLD are 8 m and 22 m, while the corresponding observed values are 13 m and 27 m in July and October, respectively. The simulated thermocline intensity are 1.2℃/m and 0.5℃/m in July and October, respectively, which are 0.6℃/m less than those of the observations. It may be the main reason why the simulated thermocline is weaker than the observations that the model vertical resolution is less precise than that of the CTD data which is 1 m. Contours of both simulated and observed thermocline intensity present a circle in general. The wave-induced mixing plays a key role in the formation of the upper mixed layer in spring and summer. Tidal mixing enhances the thermocline intensity. Buoyancy-driven mixing destroys the thermocline in autumn and keeps the vertical temperature uniform in winter.

Key words: thermocline, the Yellow Sea, wave-tide-circulation coupled model, wave-induced mixing, tidal mixing

1 INTRODUCTION

An important hydrographic feature of the Yellow Sea is the seasonal variability of the thermocline in this semi-enclosed basin (Fig.1). It has been confirmed by many observations that thermocline occurs in spring, matures in summer, diminishes in autumn and vanishes in winter. However, all the coastal circulation models face some common problems such as weaker simulated summer thermocline, and shallower depth of the upper mixed layer, comparing to the observations (Martin, 1985; Kantha and Clayson, 1994; Ezer, 2000). In this work, the MLD is regarded as upper boundary of the thermocline, and the thermocline intensity is defined as the maximum vertical temperature gradient.

As is known to all, vertical mixing process, circulation and the thermal structure influence on each other. Princeton Ocean Model (POM) employs the level 2.5 turbulence closure model to provide vertical mixing coefficients (Mellor and Yamada, 1982), which is one of the most important reasons why POM is widely accepted all over the world (Blumberg and Mellor, 1987; Ezer, 2000). Other methods, such as Prandtle mixing length theory (Fang and Ichiye, 1983), are also adopted to describe the circulation turbulence mixing. Because the mixing length on the surface is regarded zero (Mellor and Yamada, 1982), the vertical kinematic viscosity and diffusivity are weak near surface layer and zero at surface. Yuan (1979) suggested that wave-induced mixing is main process in the formation of the Yellow Sea Cold Water Mass and the related thermocline. Craig and Banner (1994) and Mellor (2003) suggested that surface waves could enhance the vertical mixing of the upper ocean. However, parameterization of wave-induced mixing for three-dimensional circulation models remains a challenge. Based on the wave-current coupled model suggested by Yuan et al. (1999), the MASNUM wave-circulation coupled model was developed (Qiao et al, 2004 a,b,c) and a wave-induced mixing term Bv was postulated as a function of wave number spectrum. The preliminary

* Supported by the National Basic Research Program of China (G1999043809) and the National Science Foundation of China (No. 49736190).

simulation experiments indicate that the upper 100 m of the Pacific and the Atlantic simulation along 35°N is much improved (Qiao et al, 2004a).

In the coastal area, the tidal current is so strong that it can enhance the vertical viscosity and diffusivity (Lee and Beardsley, 1999). The tidal mixing effect can be included into an ocean circulation model by adding the tidal current in the circulation model or parameterizing the tidal effects (Yuan and Li, 1993). Based on the wave-circulation coupled numerical model (Qiao et al, 2004 a, c), at the level of wave number spectrum, the MASNUM wave-tide-circulation coupled numerical model of the Bohai Sea, the Yellow Sea and the East China Sea is setup by adding the tidal forcing at the open boundary (Qiao et al, 2004b). The preliminary analysis focuses on the 36°N of the Yellow Sea.

Much work has been done on the circulation of the Yellow Sea (Yuan and Li, 1993; Hu et al 1991), but no work on the evolution of the thermocline in the Yellow Sea has been reported. Qi and Su (1998) set up a numerical model to evaluate the effect of tidal mixing, but they simulated for only three executive days. It is still a challenge to simulate the seasonal variability of the thermocline in the Yellow Sea with heat flux as surface boundary condition directly.

In this paper, the thermocline of the Yellow Sea is simulated and compared with the observations. The following section describes the numerical models and datasets. Section 3 compares the simulations with observations and discusses how the vertical mixing process influences the thermocline. The last section is conclusions.

2 NUMERICAL MODELS AND DATASETS

2.1 Wave model

This work employs the MASNUM (once called LAGFD-WAM) wave number spectral model (Yuan et al., 1991) which has been accepted in ocean engineering (Yu et al., 1997; Qiao et al., 1999). The model domain is (23-41°N, 117-132°E) with the horizontal resolution of 1°/6 by 1°/6 (Fig. 1). The wind fields are interpolated into the model grids from NCEP (National Centers for Environmental Prediction, USA) reanalyzed data (2001) with horizontal resolution of 1.25° by 1.0° and time interval of 6 hours.

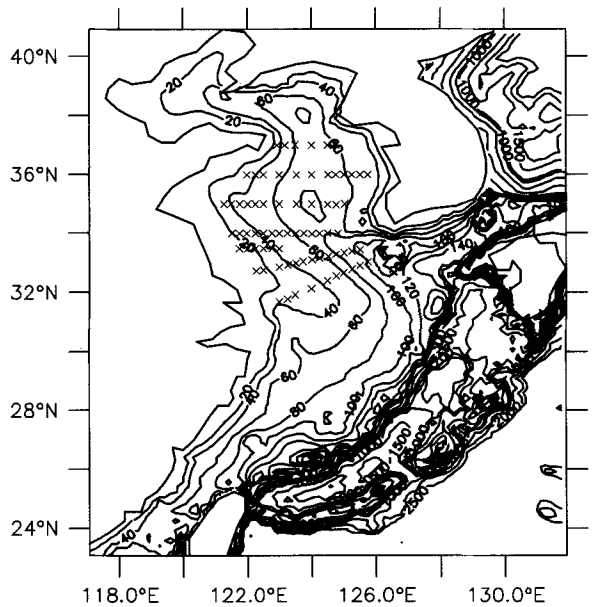

Fig. 1 Model domain and topography. Contour interval is 20 m from 0 to 200 m, 100 m from 200 to 1000 m, and 500 m from 1000 to 3000m. Crosses are the positions of in situ observation from China-Korea joint cruises

2.2 MASNUM wave-tide-circulation coupled model

Princeton Ocean Model (POM) is adopted in the present work with the wave-induced vertical mixing added directly by,

$$Km = Km_C + Bv,\ Kh = Kh_C + Bv \qquad (1)$$

where Km and Kh are the vertical viscosity and diffusivity respectively used in the model, Km_C and Kh_C are calculated by Mellor-Yamada turbulence closure model (Mellor and Yamada, 1982) and Bv is an additional term obtained from the MASNUM wave-current coupled model (Qiao et al, 2004a).

$$Bv = \alpha \iint_{\vec{k}} E\left(\vec{k}\right) \exp\{2kz\}\, d\vec{k}\, \frac{\partial}{\partial z} \left(\iint_{\vec{k}} \omega^2 E\left(\vec{k}\right) \exp\{2kz\}\, d\vec{k} \right)^{1/2} \qquad (2)$$

where $E\left(\vec{k}\right)$ represents the wave number spectrum; ω, the wave angular frequency; $\vec{k}$, wave number; and z is the vertical coordinate axis downward positive with $z = 0$ at the surface. Here we set the coefficient $\alpha = 1$.

The simulation domain is the same as the wave model. The maximum water depth is set as 3000 m (Fig. 1) and 16 vertical layers with fine resolution in

the upper layers are summarized in Table 1. NCEP (2001) offers the sea surface force. Heat flux (Q) and the evaporation minus precipitation (E-P) are from COADS (1994). Q is modified by using the Harney equation (Harney, 1971). Scheme provided by POM2k, the E-P is added as an equivalent surface salinity flux (Qiao et al, 2004b).

Table 1 Vertical layers of the circulation model

Layers	σ	Layers	σ
1	0.00000	9	-0.30000
2	-0.00313	10	-0.40000
3	-0.00625	11	-0.50000
4	-0.01250	12	-0.60000
5	-0.02500	13	-0.70000
6	-0.05000	14	-0.80000
7	-0.10000	15	-0.90000
8	-0.20000	16	-1.00000

The initial and open boundary conditions of salinity are from the Levitus (1982) data set, and those of temperature, and the initial condition of velocity are from the North Pacific simulation results of Xia et al. (2004). The eight tidal components of K_2, M_2, N_2, S_2, K_1, O_1, P_1, Q_1, are added at the lateral boundaries (Ma and Qiao, 2004)

The Changjiang (Yangtze River) diluted water is included as an across basin boundaries (Ma and Qiao, 2004) by using the monthly averaged discharge from a 37-year record at the Datong observation station (Table 2).

Three cases, 1) with both Bv and tidal mixing; 2) with Bv tidal mixing but; 3) with neither Bv nor tidal mixing, have been simulated for five executive years for stability and the results of the sixth year are compared with the observations.

Table 2 Climatological monthly mean discharge of the Changjiang (Yangtze) River (units: m^3s^{-1})

January	February	March	April	May	June	July	August	September	October	November	December
11008	11903	16825	25254	33345	40342	52183	44065	39315	32952	21817	13413

2.3 Datasets

Two datasets were used in this work: In-situ CTD data collected by the China-Korea joint cruises in October 1996 and July 1997, and Levitus (1982) dataset.

3 DISCUSSION

3.1 The evolution of the MLD

The MLD where the temperature differs from the SST by 0.5°C was regarded as the upper boundary of the thermocline. July and October were chosen as representatives of summer and autumn, respectively. The spatial distributions of simulated and observed MLD are shown in Fig. 2. In July, the observed MLD was higher in the central Yellow Sea at about 10 m and lower in the surrounded area (Fig. 2b). The simulated results showed the same pattern (Fig.2a) but the MLD was about 4 m shallower than the observations. The monthly mean wind speed in July from NCEP was about 1.5m/s less than that from Atlas of the Yellow Sea, and the wave breaking-induced vertical mixing was not included in this work. Underestimated wave-induced vertical mixing may be the reason of the underestimating of MLD. In October, the observed MLD was about 25 m (Fig. 2d) while the simulated value was about 21 m (Fig. 2c). At the edge of the Yellow Sea Cold Water Mass, the MLD increases sharply and temperature is nearly vertically uniform because strong tidal mixing can reach the surface area.

The simulated and observed MLD is shown in Fig.3. They have the same tendency in general. In July, the observed maximum MLD reached 13 m while the simulated maximum was 8 m. The simulated MLD is shallower than the observations in most area except in some locations (Fig.3a). The simulated MLD is also compared with Levitus dataset (Fig.3b).

3.2 The thermocline intensity in the Yellow Sea

It should be notified that the CTD data had high vertical resolution of 1 m, but the model resolution was much coarser in the thermocline area (Table 1), which could lead to a weaker simulated thermocline. Fig.4 shows the spatial distributions of the simulated and observed thermocline intensity in July (Figs. 4a and 4b) and October (Figs. 4c and 4d), respectively. In July, the simulated thermocline intensity reached 1.2℃/m in the western area of the Yellow Sea and 0.9℃/m in the eastern area. Its contour had a circle pattern. The observations also show these two characteristics, but they were stronger than those of the simulation. In October, the simulated and observed maximum thermocline intensity locates in the southwest area and reached 0.5℃/m and 2.0℃/m, respectively.

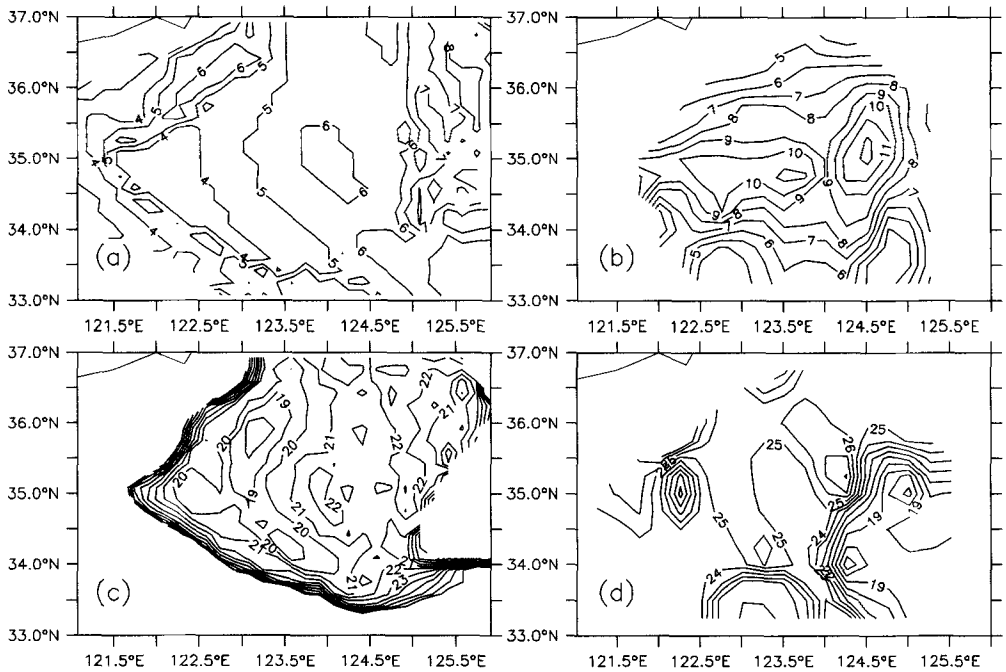

Fig. 2 Distributions of the simulated (a,c) and observed (b,d) MLD (The bottom of the mixed layer is found from the depth where the temperature differs from the SST by 0.5°C). a,b is for July and c,d is for October

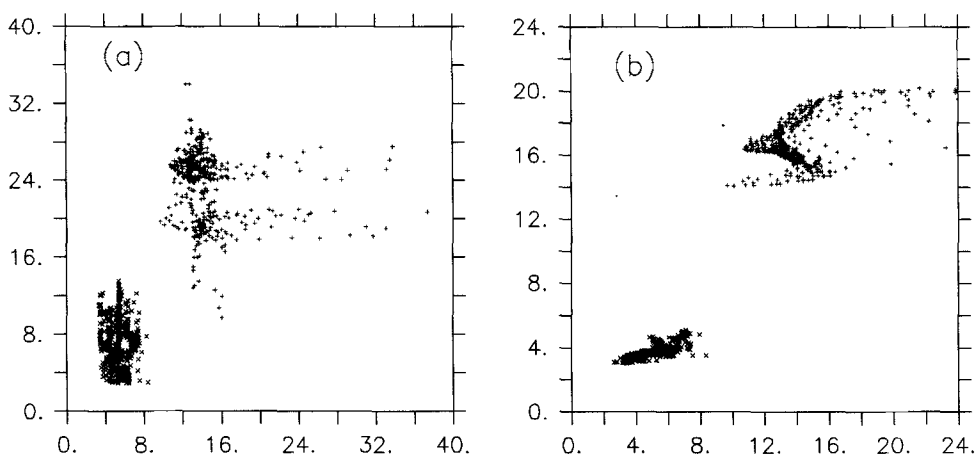

Fig. 3 Comparison of the simulated (horizontal axis) and observed (vertical axis) MLD, from a) in situ observations by China-Korea joint cruise and b) Levitus dataset. (signs of cross and plus are for July and October respectively)

3.3 Annual cycles

Evolution of MLD along 35°N in the Yellow Sea indicates that the thermocline appears at the beginning of April (Fig.5) and the MLD varies between 4-8 m from April to September. From October, the SST drops sharply and the buoyancy driven vertical mixing enlarges the MLD. In the evolution of the thermocline intensity (Fig. 6), one can find that thermocline appears at the beginning of April, develops until the beginning of June, and keeps the mature status of 1.0 °C/m or so between early June and early August. At June 5, thermocline in the eastern area is stronger than that of the western area. In August, the vertical temperature gradient can reach 1.0℃/m at the area centered (35°N, 125.5°E). From October, thermocline vanishes from the coastal area and maintains in the central area till the end of November.

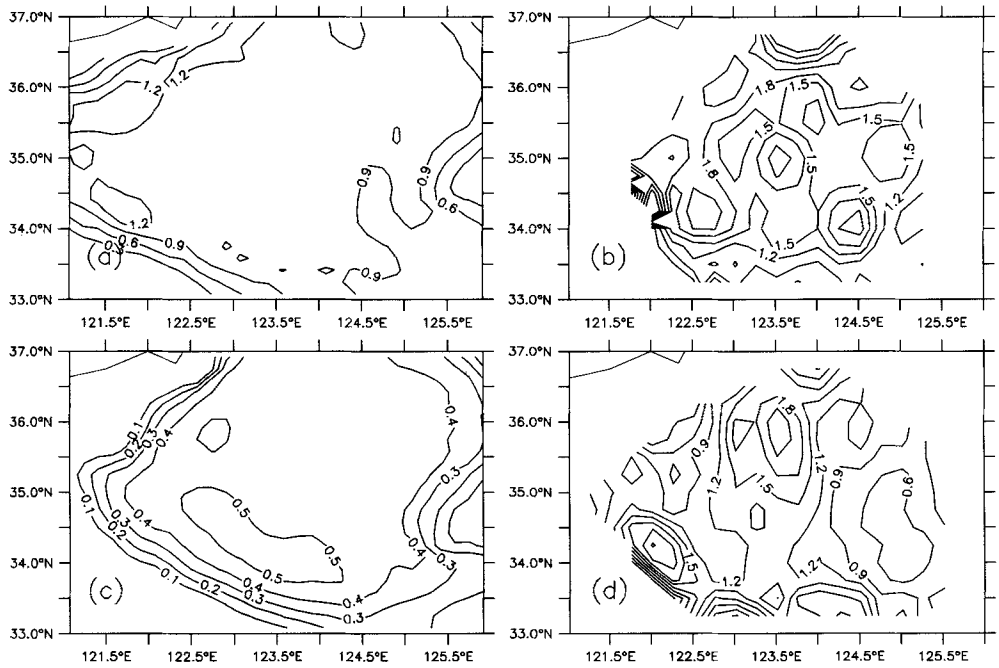

Fig. 4 Distributions of the simulated (a,c) and observed (b,d) thermocline intensity (units: ℃/m)
a,b is for July and c,d is for October

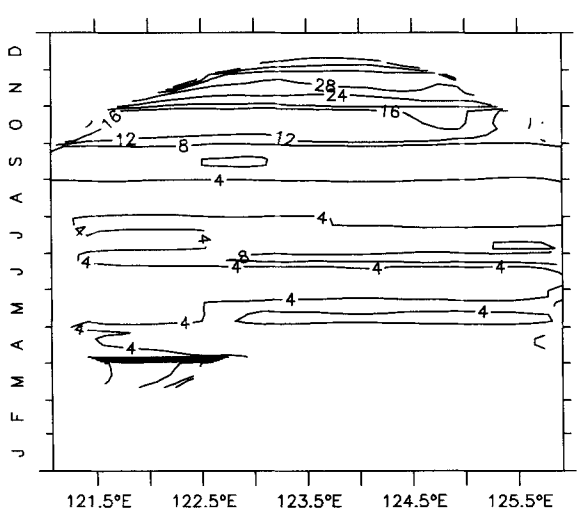

Fig. 5 Simulated annual cycle of MLD along 35°N in the Yellow Sea (units: m)

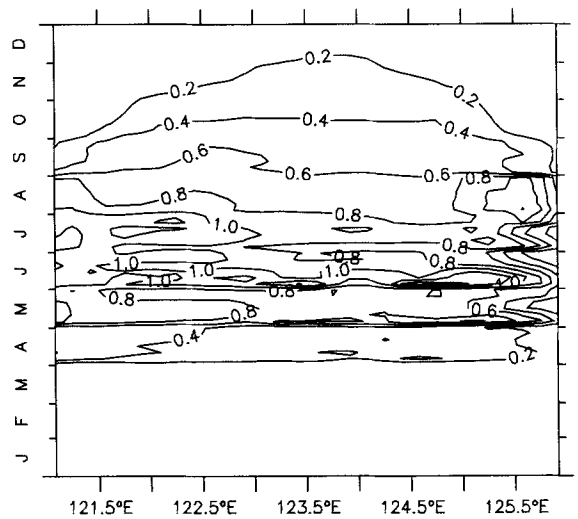

Fig. 6 Simulated annual cycle of the thermocline intensity along 35°N in the Yellow Sea (units: ℃/m)

3.4 Mechanism analysis

In order to analysis the effect of vertical mixing on the thermocline, three numerical experiment results are shown. We select two points at (35°N, 124°E) and (38°N,124°E) to represent the southern and northern Yellow Sea, respectively. Evolutions of the two points show similar patterns. The MLD is very shallow and the thermocline is very weak in summer season in the cases of no wave-induced mixing and no tidal mixing (Fig. 7a, d), which are the common problems of all ocean numerical models (Martin, 1985; Ezer, 2000). In the case with wave-induced mixing but tidal mixing, the MLD is enlarged (Fig.7b, e). Since the tidal mixing affects mainly the area within 30 m from the bottom (Qiao et al, 2004b), it makes the vertical temperature gradients a little stronger (Fig. 7c, f).

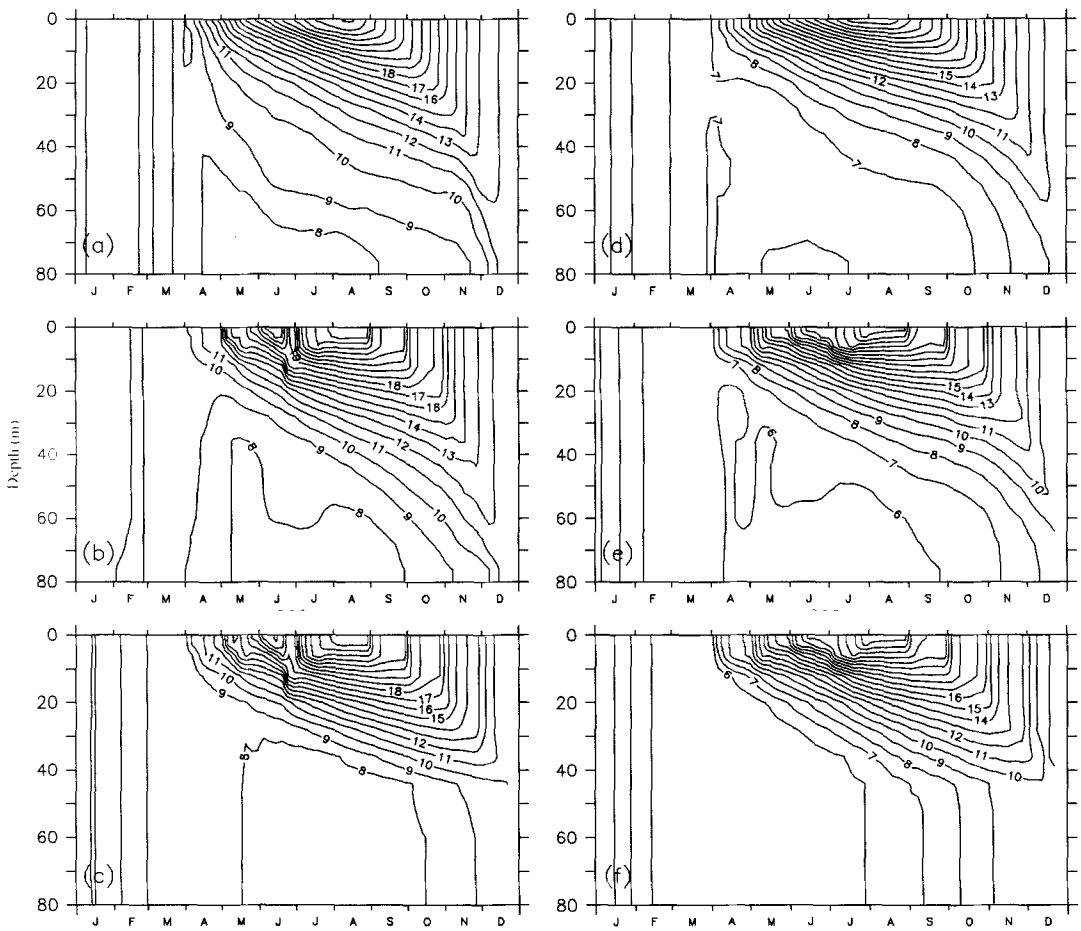

Fig. 7 Annual cycles of the temperature at (35°N, 124°E) (a,b,c) and (38°N, 124°E) (d,e,f) which locate at the center of the Southern and Northern Yellow Sea respectively

a,d: neither wave-induced mixing nor tidal mixing; b,e: with wave-induced mixing but tidal mixing; c,f: with wave-induced mixing and tidal mixing

4 CONCLUSIONS

1. Based on the MASNUM wave- tide- circulation coupled numerical model, the evolution of the thermocline in the Yellow Sea is simulated and compared with the observations. Simulated results suggest that the ability to simulate the thermocline is much improved by the MASNUM coupled numerical model. The simulated MLD and the thermocline intensity in the Yellow Sea have similar spatial patterns with the observations in July and October, though the simulated MLD is a little shallower and the thermocline intensity is somewhat weaker, which may be caused by underestimated wind stress, omitting of the wave breaking induced vertical mixing, and coarse vertical resolution.

2. Three cases of numerical experiments indicate that wave-induced vertical kinematic viscosity (or diffusivity) plays a key role in the formation of the upper mixed layer and thermocline. Tidal current induced mixing can enhance the thermocline intensity in summer. In late autumn and winter, it is the buoyancy-driven vertical mixing who makes the vertical temperature uniform.

References

Blumberg, A. F. and G. L. Mellor, 1987. A description of a three-dimensional coastal ocean model. *In:* N. S. Heaps, ed, Three dimensional coastal ocean models, American Geophysical Union, Washington D. C., p. 1-16.

Craig, P. D. and M. L. Banner, 1994. Modeling wave-enhanced turbulence in the ocean surface layer. *J. Phys. Oceanogr.* **24**: 2546-2559.

Ezer, T., 2000. On the seasonal mixed layer simulated by a basin-scale ocean model and the Mellor-Yamada turbulence scheme. *J. Geophys. Res.* **105** (C7): 16843-16855.

Fang, G. and T. Ichiye, 1983. On the vertical structure of

tidal currents in a homogeneous sea. *Geophys. J. R. Astr. Soc.* **73**: 65-82.

Harney, R., 1971. Surface thermal boundary condition for ocean circulation models. *J. Phys. Oceanogr.* **1:** 241-248.

Hu, D., M. Cui, Y. Li and T. Qu, 1991. On the Yellow Sea cold water mass related circulation. *Yellow Sea Researc.* **4**: 79-88.

Kantha, L. H. and C. A. Clayson, 1994. An improved mixed layer model for geophysical applications. *J. Geophys. Res.* **99**: 25235-25266.

Lee, S. H. and R. C. Beardsley, 1999. Influence of stratification on residual tidal currents in the Yellow Sea. *J. Geophys. Res.* **104**(C7), 15679-15701.

Levitus, S., 1982. Climatological atlas of the world ocean. NOAA Prof. Paper No. 13. U. S. Govt. Printing Office, 173 pp. plus 17 microfiche.

Ma, J. and F. Qiao, 2004. Simulation and analysis on the seasonal variability of salinity in the Yellow Sea. *Chinese J. Oceanol. Limnol.* **22**(3): 306-313.

Martin, P. J., 1985. Simulation of the mixed layer at OWS November and Papa with several models. *J. Geophys. Res.* **90:** 581-597.

Mellor, G. L., 2001. One-dimensional, ocean surface layer modeling. a problem and a solution. *J. Phys. Oceanogr.* **31**: 790-809.

Mellor, G., 2003. The three-dimensional current and wave equations. *J. Phys. Oceanogr.* **33**: 1978-1989.

Mellor, G. L. and T. Yamada, 1982. Development of a turbulence closure model for geophysical fluid problems. *Rev. Geophys. and Space Phys.* **20**: 851-875.

Qi, J. and Y. Su, 1998. Numerical simulation of the tide-induced continental front in the Yellow Sea. *Oceanol. et Limnol.* **29**(3): 247-254. (in Chinese with English abstract)

Qiao, F., S. Chen, C. Li, W. Zhao and Z. Pan, 1999. The study of wind, wave, current extreme parameters and climatic characters of the South China Sea. *Journal of Marine Technology Society* **33** (1): 61-68.

Qiao, F., Y. Yuan, Y. Yang, Q. Zheng, C. Xia and J. Ma, 2004a. Wave-induced mixing in the upper ocean: Distribution and application to a global ocean circulation model. *Geophys. Res. Lett.* **31:** L11303, doi: 10.1029/ 2004GL019824.

Qiao F., J. Ma, Y. Yang and Y. Yuan, 2004b. Simulation of the temperature and salinity along 36°N in the Yellow Sea with a wave-current coupled model. *Journal of the Korean Society of Oceanography.* **39**(1): 35-45.

Qiao, F., Y. Yuan, T. Ezer, C. Xia, Y. Yang and J. Ma, 2004c. A three-dimensional, surface wave-ocean circulation coupled model: System description and initial testing. *J. Phys. Oceanogr.* (Submitted)

Xia, C., F. Qiao and Y. Yuan, 2004. Numerical simulation of the general circulation. Submitted to *Chinese Journal of Computational Physics.* (in Chinese)

Yu, W., F. Qiao, Y. Yuan and Z. Pan, 1997. Numerical modeling of wind and waves for Typhoon Betty (8710). *Acta Ocenol. Sin.* **16** (4): 459-473.

Yuan, Y., Z. Pan, F. Hua, L. Sun, 1991. LAGDF-WAM numerical wave model. *Acta Ocenol. Sin.* **10:** 483-488.

Yuan Y. 1979. The circulation of the Yellow Sea Cold Water Mass. *Oceanol. et Limnol. Sin.* **10:** 187-196.

Yuan, Y., F. Qiao, F. Hua and Z. Wan, 1999. The development of a coastal circulation numerical model: 1. Wave-induced mixing and wave-current interaction. *J. Hydrodynamics*, Ser. A. **14**(4B): 1-8. (in Chinese)

Yuan, Y. and H. Li, 1993. Research on the circulation structure and forming mechanism of the Yellow Sea cold water mass. *Science in China* **23** (1): 93-103. (in Chinese)